Synthesis P. Vízcaíno-Milla et al. Special Topic

Primary Amine–2-Aminopyrimidine Chiral Organocatalysts for the Enantioselective Conjugate Addition of Branched Aldehydes to Maleimides

Pascuala Vízcaíno-Milla[a]
José M. Sansano[a]
Carmen Nájera*[a]
Béla Fiser[b]
Enrique Gómez-Bengoa*[b]

[a] Departamento de Química Orgánica and Centro de Innovación, en Química Avanzada (ORFEO-CINQA), Universidad de Alicante, Apdo. 99, 03080 Alicante, Spain
cnajera@ua.es
[b] Departmento de Química Orgánica I, Facultad de Química, Universidad del País Vasco, Apdo. 1072, 20080 San Sebastián, Spain
enrique.gomez@ehu.es

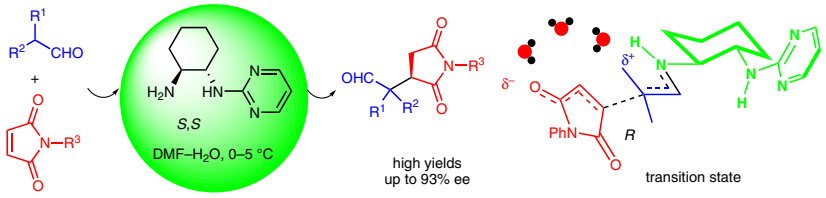

Received: 26.03.2015
Accepted after revision: 13.04.2015
Published online: 26.05.2015
DOI: 10.1055/s-0034-1380718; Art ID: ss-2015-c0196-st

Abstract Chiral primary amines containing the (*R*,*R*)- and (*S*,*S*)-*trans*-cyclohexane-1,2-diamine scaffold and a pyrimidin-2-yl unit are synthesized and used as general organocatalysts for the Michael reaction of α-branched aldehydes to maleimides. The reaction takes place with 10 mol% organocatalyst loading and hexanedioic acid as cocatalyst in aqueous *N*,*N*-dimethylformamide at 10 °C affording the corresponding succinimides in good yields and enantioselectivities. DFT calculations support the stereochemical results and the role played by the solvents.

Key words asymmetric organocatalysis, maleimides, succinimides, aldehydes, Michael addition

Enamine[1] and iminium[2] activation modes of carbonyl compounds have promoted the development of asymmetric organocatalysis in the last 15 years. Initially chiral secondary amines were used predominantly in amino catalysis, but more recently primary amines have appeared that are based on the chemistry of type I aldolases with lysine residues.[3] Chiral primary amines derived organocatalysts are crucial for enamine formation of hindered carbonyl compounds, namely α,α-disubstituted aldehydes.[4] Several problems have to be overcome with α-branched aldehydes apart from steric hindrance,[5] the formation of low reactive enamines,[6] and *Z*/*E* mixture of diastereomeric enamines. Several enantioselective reactions have been performed, such as conjugate additions, aldol and Mannich reactions, and α-heterofunctionalization of aldehydes, allowing the formation of quaternary stereocenters.

Apart from amino acid derivatives, several bifunctional primary amine organocatalysts derived from chiral 1,2-diamines have been developed. Among them, *trans*-cyclohexane-1,2-diamine, available in both enantiomeric forms, is an excellent rigid chiral scaffold to anchor a moiety able to activate the electrophile by hydrogen bonding lowering the LUMO.[7] Since the pioneering studies performed by Jacobsen,[8] Schreiner,[9] and Takemoto,[10] primary amine-thiourea derivatives have become the most popular organocatalysts.[4b,c]

Organocatalyzed conjugate addition of α,α-disubstituted aldehydes to maleimides is one of the most studied reactions using primary amine catalysts. This process allows easy access to enantiomerically substituted succinimides, which are interesting core structural units in natural products and biologically active compounds, such as andrimid, moiramide B, and hirsutellones A–E with antibacterial activity, haterumaimides A–Q with antitumor activity, and tandospirone, which is an anxiolytic and antidepressant drug.[11] In addition, enantioenriched succinimides can be used as chiral building blocks as they are easily transformed into pyrrolidines, γ-lactams, and γ-lactones.[12]

Bifunctional primary amine derived organocatalysts from *trans*-cyclohexane-1,2-diamine (*R*,*R*)-**1** and its enantiomer, bearing a thiourea unit **2**,[13] **3**,[14] the guanidine derivative **4**,[15] the starting diamine **1**,[16] and its *N*-Boc-monoprotected derivative **5**,[17] efficiently promoted the Michael-type addition of α,α-disubstituted aldehydes to maleimides (Figure 1). Recently, we demonstrated that the 2-aminobenzimidazole[18] and 2-aminopyrimidine[19] units are excellent hydrogen bond donors, the corresponding bifunctional organocatalysts **6**[18] and **7**[19] were used in Michael and aldol reactions, respectively (Figure 1).

Continuing this line of research, and based on the experience of our group in organocatalyzed asymmetric reactions, we envisaged that a primary amine–2-aminopyrimidine organocatalyst **8** derived from *trans*-cyclohexane-1,2-

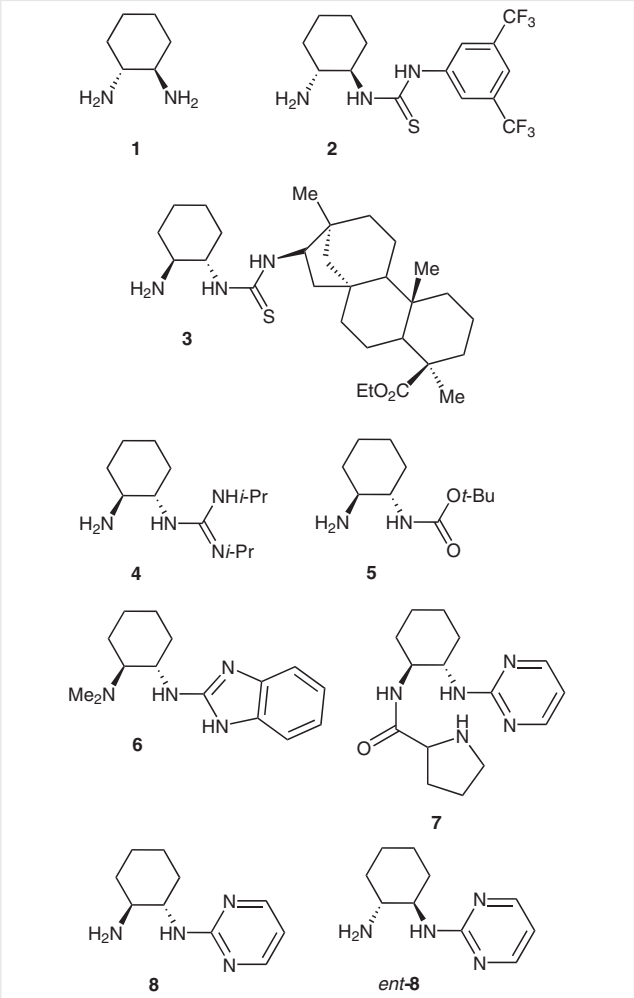

Figure 1 *trans*-Cyclohexane-1,2-diamine-derived organocatalysts

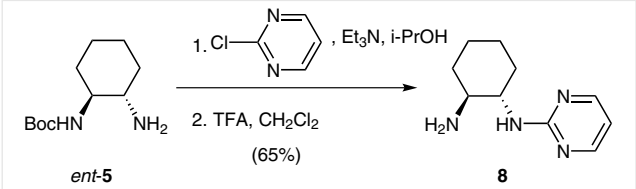

Scheme 1 Synthesis of the organocatalyst **8**

diamine would be able to catalyze the conjugate addition of α,α-disubstituted aldehydes to maleimides. Density functional theory (DFT) calculations would clarify the role of the 2-aminopyrimidine unit as rigid guanidine-type function able to form hydrogen bonds with the carbonyl group of the maleimide acceptor.

The primary amine–aminopyrimidine organocatalyst **8** was synthesized by reaction of *N*-Boc-monoprotected derivative *ent*-**5** with commercially available 2-chloropyrimidine in the presence of triethylamine in refluxing propan-2-ol for 36 hours, followed by trifluoroacetic acid deprotection at room temperature in dichloromethane (Scheme 1).[19] Compound **8** and its enantiomer *ent*-**8** were both obtained in 65% overall yield.

As model reaction isobutyraldehyde (2 equiv) was reacted with *N*-phenylmaleimide in the presence of 10 mol% of organocatalyst **8** (Table 1). When the reaction was performed in toluene as the solvent at room temperature for three days the corresponding succinimide **9a** was isolated in 78% yield as a racemic compound (entry 1). Under the same reaction conditions using tetrahydrofuran instead of toluene the reaction failed, and in dichloromethane compound **9a** was isolated in 79% yield with a modest 29% ee and with *S*-configuration (entries 1–3). However, the use of water as the solvent gave **9a** after three days in 74% yield and with 44% ee with *R*-configuration (entry 4). The same sense of enantiomeric bias was observed in *N*,*N*-dimethylformamide, but longer reaction times (ca. 6 d), lower yield (33%), and higher enantiomeric excess (62% ee) (entry 5). Therefore, mixtures *N*,*N*-dimethylformamide–water (in ratios of 2:1 and 4:1) were examined and these afforded similar results, 70% yield and 79% ee (entries 6 and 7).

The reaction failed in the presence of basic additives such as DABCO or imidazole (entries 8 and 9), which were beneficial in the case of organocatalysts **1**[16] and **4**.[15] On the other hand, when carboxylic acids such as trifluoroacetic, benzoic, or hexanedioic acid, were used as the additive, the reaction accelerated only in the case of benzoic and hexanedioic acids (entries 10–12). Using 10 mol% hexanedioic acid as the cocatalyst gave product (*R*)-**9a** in 80% yield and with 79% ee; 20 mol% loading of catalyst and cocatalyst gave the same results (entry 13). Using *ent*-**8** as the catalyst gave the corresponding product (*S*)-**9a** (entry 14).

Finally, when the temperature was lowered to 0 °C, the time required for the reaction to go to completion was two days giving the product in 83% isolated yield and with 88% ee (entry 15). Under the latter reaction conditions, this conjugate addition of isobutyraldehyde was scaled up from 0.3 mmol to ca. 3.5 mmol [*N*-phenylmaleimide (0.5 g)] affording (*R*)-**9a** after 16 hours reaction time in 99% crude yield and with 85% ee. Further recrystallization from hexane–ethyl acetate gave pure succinimide in 75% yield.

Once the optimal reaction conditions had been established [catalyst **8** (10 mol%), hexanedioic acid (10 mol%) as cocatalyst, in *N*,*N*-dimethylformamide–water (2:1) as solvents, at 0 to 5 °C], the scope of the reaction was studied (Scheme 2). The addition of isobutyraldehyde to maleimide and *N*-alkylmaleimides such as *N*-methyl- and *N*-benzylmaleimide, afforded succinimides **9b**–**d** in good yields and 76–82% ee. In the case of the conjugate addition of isobutyraldehyde to *N*-aryl-substituted maleimides the corresponding products **9e**–**g** were obtained in higher yields (70–92%) and with 87–86% ee (Scheme 2).

Table 1 Optimization of the Reaction Conditions[a]

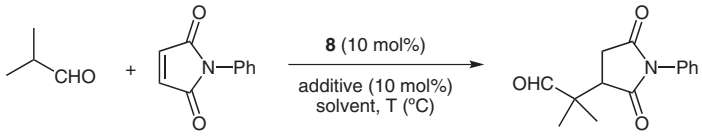

9a

Entry	Solvent	Additive	Temp (°C)	Time (h)	Yield[b] (%)	ee[c] (%)
1	toluene	–	25	72	78	*rac*
2	THF	–	25	96	–	–
3	CH_2Cl_2	–	25	72	79	29 (*S*)
4	H_2O	–	25	72	74	44 (*R*)
5	DMF	–	25	140	33	62 (*R*)
6	DMF–H_2O (2:1)	–	25	72	70	79 (*R*)
7	DMF–H_2O (4:1)	–	25	72	71	79 (*R*)
8	DMF–H_2O (2:1)	DABCO	25	72	–	–
9	DMF–H_2O (2:1)	imidazole	25	72	–	–
10	DMF–H_2O (2:1)	TFA	25	72	–	–
11	DMF–H_2O (2:1)	$PhCO_2H$	25	16	84	75 (*R*)
12	DMF–H_2O (2:1)	HDA[d]	25	16	80	79 (*R*)
13	DMF–H_2O (2:1)	HDA[e]	25	15	80	79 (*R*)
14[f]	DMF–H_2O (2:1)	HDA[e]	25	18	77	79 (*S*)
15	DMF–H_2O (2:1)	HDA[e]	0	48	83	88 (*R*)

[a] Reaction conditions: isobutyraldehyde (0.6 mmol), *N*-phenylmaleimide (0.3 mmol), catalyst **8** (10 mol%), additive (10 mol%), solvent (0.6 mL).
[b] Isolated yield after flash chromatography.
[c] Determined by chiral HPLC.
[d] Hexanedioic acid.
[e] 20 mol%.
[f] The reaction was carried out using *ent*-**8**.

In order to extend this methodology to other aldehydes such as cyclopentane- and cyclohexanecarbaldehyde were allowed to react with *N*-phenylmaleimide. The resulting succinimides **9h** and **9i** were isolated in 84 and 89% yield and with 89 and 93% ee, respectively (Scheme 2). Low diastereoselectivity was observed in the Michael addition of 2-phenylpropanal and propanal giving products **9j** and **9k** in 72 and 49% yields and as a mixture 6:1 and 2:1 of diastereomers, respectively; the major isomers **9j** and **9k** were obtained with 81% and 72% ee, respectively.

The absolute configuration was assigned according to our previous work using **4** as an organocatalyst.[15] The observed enantioinduction indicates that the catalytic process should take place through a different activation mode of the 2-aminopyrimidine than the thiourea unit in Takemoto's catalyst **2**.[13b] Experimental work using catalyst **8** with different enantiomeric excess revealed the absence of a nonlinear effect, it means that in the transition state only one molecule of the catalyst is involved.

In addition, DFT calculations were carried out in order to get a deeper understanding into the origin of the enantioselectivity with catalyst **8**, for the reaction between isobutyraldehyde and *N*-phenylmaleimide. Considering that the bifunctional catalyst **8** bears primary and secondary amine moieties, the classical mechanism supports the formation of a nucleophilic reacting enamine from the primary amine and aldehyde. At this point it is reasonable that this intermediate enamine attacks one of the enantiotopic faces of the maleimide electrophile. As expected, our preliminary studies showed that this attack is in agreement with the Seebach's synclinal model (Figure 2).[20] A key feature of this model is that the reacting face of the enamine diastereospecifically attacks only one of the faces of the maleimide. That is, the lower face of the enamine (from our point of view in Figure 2) is reacting with the *Re* face of the maleimide, and the upper face of the enamine must react with the *Si* face of the maleimide. The transition structures found in the present study follow this simple reactivity model.

The most intriguing experimental data is the solvent-dependent sense of the enantioselectivity, which affords the major *R*-enantiomer in a highly polar reaction medium (DMF–H_2O), a racemic mixture in toluene, and the reversal

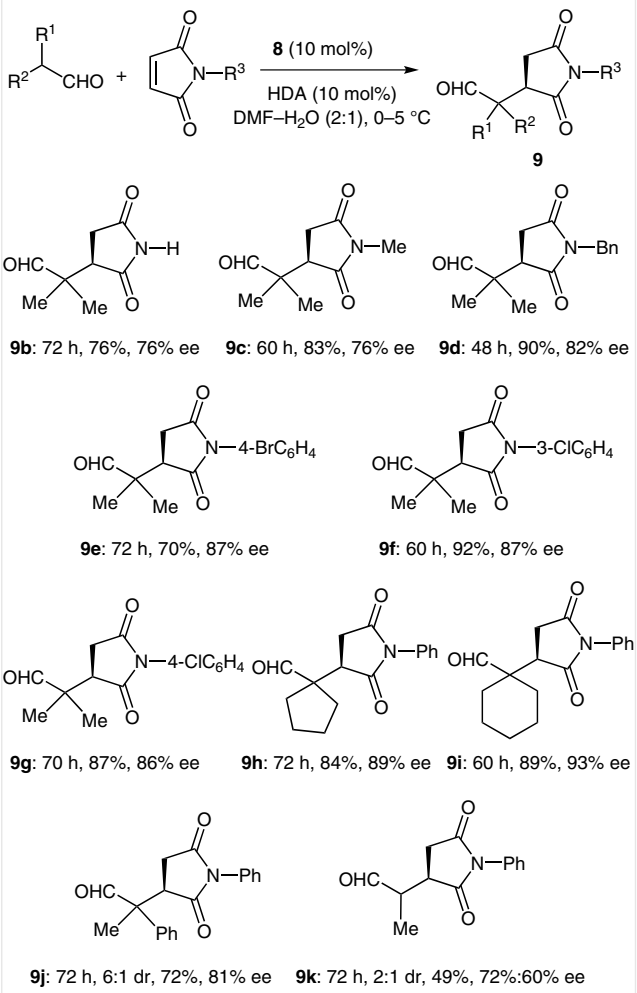

Scheme 2 Synthesis of enantioenriched succinimides **9**

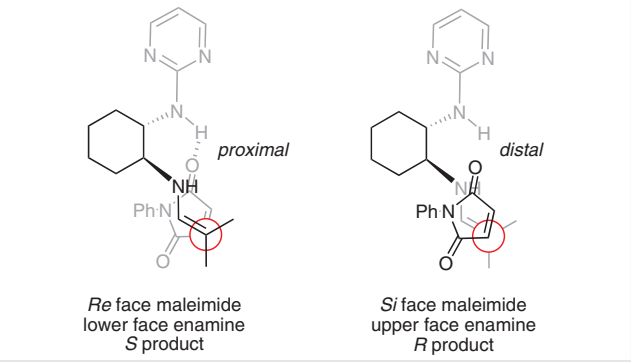

Figure 2 Faces of enamine and *N*-phenylmaleimide reacting through Seebach's synclinal model

formation of *S*-product (although with low ee) in a more apolar solvent such as dichloromethane. Our computational data provide a plausible explanation of this interesting effect.

At first glance, the secondary NH moiety of the aminopyrimidine group seems to be well suited to H-bond activation of the maleimide carbonyl oxygen, which could lower the activation energy of the reaction and increase the reaction rate. Our initial hypothesis is that the model structure on the left in Figure 2 (*Re* face of the maleimide) shows a better disposition of the maleimide and the aminopyrimidine fragments to interact by H-bonding, since they are both found quite close to each other in the lower face of the enamine. Thus, apolar and nonprotic solvents that favor the formation of such internal H-bonds, would induce the generation of the *S*-enantiomer. In the inverse situation, the transition state leading to the formation of the *R*-enantiomer (Figure 2, right) does not show a facile H-bonding pattern, since the pyrimidine and maleimide occupy opposite faces of the enamine. This structure would be favored in polar, protic solvents that are known to easily solvate polar transition states, disrupting internal H-bond interactions.

We confirmed this hypothesis in light of the computed transition state activation energies. For example, a structure was located (TS-S_1, Figure 3), that bears the mentioned H-bond, leading to the formation of the *S*-product. It corresponds to a quite apolar TS, and therefore, the computed activation values reflect a marginal dependence on the solvent model employed during the calculations. Nonetheless, as expected, the lowest barrier corresponds to the gas phase system (15.8 kcal/mol), which also presents the strongest H-bond (2.00 Å). The H-bonding strength decreases in dichloromethane (2.03 Å), and even more in water (2.12 Å).

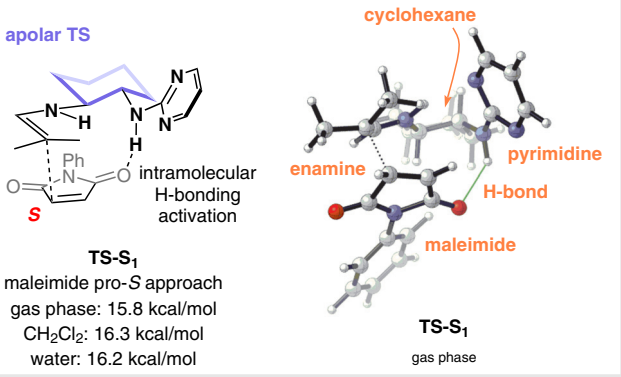

Figure 3 Computed activation energies for the transition state TS-S_1 in the gas phase, dichloromethane and water models. Structures and values were obtained at M06-2X/6-311++G** level of theory.

Furthermore, a number of transition states lacking any internal H-bond were located, and the two lowest in energy among them are shown in Figure 4. Both structures lead to the formation of the *R*-enantiomer. Their charge separation (developing negative charge in the carbonyl oxygen and positive in the enamine nitrogen) is quite high, inducing a polar structure, that would be better stabilized in polar sol-

vents. Indeed, not surprisingly, the activation energy values show a clear decreasing trend on going from the gas phase system (>17 kcal/mol), to dichloromethane (ca. 16 kcal/mol) to the lowest one in water (15.4 kcal/mol). The energy differences between gas phase and water, ca. 2 kcal/mol, are significant and could justify an increase reactivity of around two orders of magnitude. Also, the three energy values for TS-R_1 are lower than the corresponding values for TS-R_2, indicating that the former is operative in the mechanism leading to the *R*-enantiomer.

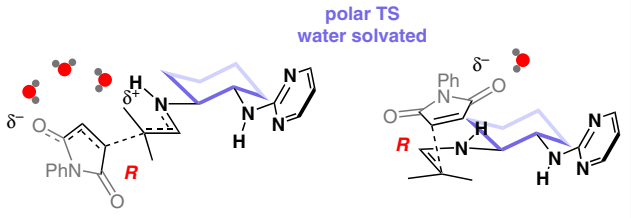

TS-R_1
maleimide pro-*R* face approach
gas phase: 17.2 kcal/mol
CH_2Cl_2: 15.9 kcal/mol
water: 15.4 kcal/mol

TS-R_2
maleimide pro-*R* approach
gas phase: 18.3 kcal/mol
CH_2Cl_2: 16.4 kcal/mol
water: 16.2 kcal/mol

Figure 4 Computed activation energies for the transition states TS-R_1 and TS-R_2 in the gas phase, dichloromethane and water models. Structures and values were obtained at M06-2X/6-311++G** level of theory.

The main outcome of this study is that if the reaction is carried out in polar solvents such as the *N*,*N*-dimethylformamide–water mixture, any possible internal H-bond would be disrupted, resulting in the lowest activation energy (in a water model) for TS-R_1 (15.4 kcal/mol). In the opposite direction, TS-S_1, which bears an internal H-bond, is predicted to be the most favorable structure in the absolutely apolar gas phase model (15.8 kcal/mol). Both data are in agreement with the experimental trend, *R*-enantiomer in polar and *S*-enantiomer in apolar systems. The calculations in dichloromethane are between those of water and gas phase. Whilst it is true that the lowest energy value in dichloromethane *erroneously* corresponds to TS-R_1 (15.9 kcal/mol), its difference to TS-S_1 is very low (0.4 kcal/mol) and can be considered within the calculation error limits. Taking also into account that the 24% excess of *S* compound in dichloromethane corresponds to an experimental energy difference of 0.29 kcal/mol, and that the reaction in the similar solvent toluene produces racemic product, the agreement between experiment and theory at this point is also significant.

In conclusion, *trans*-cyclohexane-1,2-diamine derived primary amine–2-aminopyrimidine organocatalysts **8** promote the conjugate addition of aldehydes to maleimides with 10 mol% loading and using hexanedioic acid as cocatalyst in good yield and up to 93% ee. The best solvent is *N*,*N*-dimethylformamide and the presence of water as cosolvent has a beneficial effect on the yield, reaction time, and enantioselectivity. DFT calculations support that H-bonding activation of the maleimide by NH moiety of the aminopyrimidine is not taking place in the enantiodiscrimination stage. The aminopyrimidine unit shows only steric hindrance in the transition state. However, under apolar solvents due to H-bonding interactions the opposite enantiomer, but with very poor enantioselection, is preferred.

All reagents were purchased from commercial sources and used without further purification. Substrates which were not commercially available were synthesized according to known literature procedures. Catalysts **8** were synthesized as previously described.[19] Melting points were determined with a Reichert Thermovar hot plate apparatus and are uncorrected. IR spectra were recorded on a Jasco FT-IR 4100 LE (Pike Miracle ATR) and only the structurally most relevant peaks are listed. NMR spectra were performed on a Bruker AC-300 or Bruker Avance-400 using $CDCl_3$ as solvent and TMS as internal standard unless otherwise stated. LR-MS (EI) mass spectra were obtained at 70eV on Agilent GC/MS-5973N apparatus equipped with a HP-5MS column (Agilent technologies, 30 m × 0.25 mm) and HRMS-ESI were obtained on a Waters LCT Premier XE apparatus equipped with a time of flight (TOF) analyzer and the samples were ionized by ESI techniques and introduced through an ultra-high pressure liquid chromatography (UPLC) model Waters Acquity H class. Optical rotations were measured on a Jasco P-1030 Polarimeter with a 5-cm cell (*c* given in g/100 mL). Enantioselectivities were determined by HPLC analysis (Agilent 1100 Series HPLC) equipped with a G1315B diode array detector and a Quat Pump G1311A equipped with the corresponding Daicel chiral column. Analytical TLC was performed on Merck silica gel plates and the spots visualized with UV light at 254 nm. Flash chromatography employed prepackaged columns (12 mm i.d ×7.5 or 15 cm) using Merck silica gel 60 (0.040–0.063 mm) and a chromatography pump Büchi Controller C-610-Module C-601. Silica gel 60 F_{254} containing gypsum was employed for preparative layer chromatography.

(*S*,*S*)-2-(Pyrimidin-2-ylamino)cyclohexaneamine (8);[19] Typical Procedure

A mixture of *ent*-**5** (3.27 g, 15.25 mmol), Et_3N (2.53 mL, 18.31 mmol), and 2-chloropyrimidine (2.09 g, 18.31 mmol) in *i*-PrOH was stirred for 36 h at 80 °C under argon atmosphere. The mixture was concentrated in vacuo and the residue was dissolved in CH_2Cl_2 (10 mL) and washed with H_2O (3 × 20 mL). After removal of the solvent under reduced pressure the resulting reside was purified by flash chromatography (hexane–EtOAc) to give Boc-protected **8** (3.52 g). The resulting solid residue was dissolved in CH_2Cl_2 (110 mL) and TFA (9.08 mL, 120 mmol) was added and the mixture was stirred for 4 h. The solvents were removed under reduced pressure and the residue was dissolved in CH_2Cl_2 (30 mL) and extracted with H_2O (3 × 30 mL). The aqueous layer was treated with 2 M NaOH solution until basic pH and extracted with CH_2Cl_2 (3 × 60 mL). The combined organic layers were dried ($MgSO_4$) and filtered, and the solvents were removed under reduced pressure to yield **8** (2.64 g, 71% overall yield) as a yellow solid; mp 75°C; $[\alpha]_D^{26}$ +51.4 (*c* 1, $CHCl_3$).

IR: 3243, 2927, 2859, 1583, 1528, 1449, 1418, 1136, 959, 920, 798.

^{1}H NMR: δ = 8.22 (d, *J* = 4.8 Hz, 2 H), 6.46 (t, *J* = 4.8 Hz, 1 H), 5.65 (d, *J* = 9.1 Hz, 1 H), 3.64 (dtd, *J* = 11.2, 9.6, 4.1 Hz, 1 H), 2.46 (td, *J* = 10.5, 4.1 Hz, 1 H), 2.10–1.90 (m, 2 H), 1.75–1.62 (m, 2 H), 1.55 (br s, 2 H), 1.43–1.03 (m, 4 H).

^{13}C NMR: δ = 162.94, 158.03, 110.46, 57.67, 55.97, 35.02, 32.74, 25.27, 25.19.

HRMS (ES): *m*/*z* [M + H]$^+$ calcd for $C_6H_{16}N_4$: 193.1453; found: 193.1448.

(*R*,*R*)-2-(Pyrimidin-2-ylamino)cyclohexaneamine (*ent*-8); Typical Procedure

Following the typical procedure using **5** (3.27 g, 15.25 mmol) gave *ent*-**8** (2.64 g, 71% overall yield) as a yellow solid.

Substituted Succinimides 9; General Procedure

To a solution of **8** or *ent*-**8** (0.03 mmol), maleimide (0.3 mmol), and hexanedioic acid (0.03 mmol, 10% mol) in DMF–H_2O (2:1, 0.6 mL) was added the aldehyde (0.6 mmol) and the mixture was stirred at 0 °C until completion of the reaction (TLC) (times are given in Scheme 2). Then, aq 2 M HCl (10 mL) was added and the mixture was extracted with EtOAc (3 ×10 mL). The combined organic phases were washed with H_2O (2 × 10 mL), dried ($MgSO_4$), filtered, and evaporated (20 mbar). The resulting crude was purified by flash chromatography (*n*-hexane–EtOAc) to afford adduct **9**.

Compound **9a** was also prepared on a larger scale (starting from 0.5 g, 2.8 mmol of NPM). Isolation by recrystallization (hexane–EtOAc) led to 0.531 g (75%) of the product that maintained the same optical purity.

(*R*)-2-(2,5-Dioxo-1-phenylpyrrolidin-3-yl)-2-methylpropanal (9a)[13b]

Following the general procedure gave **9a** (68.43 mg, 93%) as colorless prisms.

HPLC [Chiralpak OD-H, 230 nm, *n*-hexane–*i*-PrOH, 70:30, 0.9 mL/min): t_R = 17.4 (minor), 22.7 min (major).

^{1}H NMR: δ = 9.52 (s, 1 H), 7.52–7.35 (m, 3 H), 7.31–7.24 (m, 2 H), 3.15 (dd, *J* = 9.5, 5.5 Hz, 1 H), 2.98 (dd, *J* = 18.2, 9.5 Hz, 1 H), 2.62 (dd, *J* = 18.2, 5.5 Hz, 1 H), 1.33 (s, 3 H), 1.29 (s, 3 H).

^{13}C NMR: δ = 202.82, 176.97, 174.85, 131.95, 129.31, 128.85, 126.66, 48.66, 45.16, 32.02, 20.44, 19.79.

(*R*)-2-(2,5-Dioxopyrrolidin-3-yl)-2-methylpropanal (9b)[15b]

Following the general procedure gave **9b** (38.53 mg, 76%) as colorless prisms; 76% ee.

HPLC (Chiralpak AD-H, 210 nm, *n*-hexane–*i*-PrOH, 85:15, 1.0 mL/min): t_R = 27.5 (major), 38.6 min (minor).

^{1}H NMR: δ = 9.49 (s, 1 H), 8.73 (br s, 1 H), 3.10 (dd, *J* = 9.4, 5.8 Hz, 1 H), 2.85 (dd, *J* = 18.4, 9.4 Hz, 1 H), 2.51 (dd, *J* = 18.4, 5.8 Hz, 1 H), 1.25 (s, 3 H), 1.23 (s, 3 H).

^{13}C NMR: δ = 202.9, 178.3, 176.2, 48.0, 46.3, 32.8, 20.1, 19.4.

(*R*)-2-Methyl-2-(1-methyl-2,5-dioxopyrrolidin-3-yl)propanal (9c)[13b]

Following the general procedure gave **9c** (45.61 mg, 83%) as a colorless oil; 76% ee.

HPLC (Chiralpak AS-H, 210 nm, *n*-hexane–*i*-PrOH, 80:20, 1.0 mL/min): t_R = 15.6 (major),17.7 min (minor).

^{1}H NMR: δ = 9.51 (s, 1 H), 3.04 (dd, *J* = 9.3, 5.4 Hz, 1 H), 2.99 (s, 3 H), 2.82 (dd, *J* = 18.2, 9.3 Hz, 1 H), 1.22 (s, 3 H), 1.21 (s, 3 H).

^{13}C NMR: δ = 202.9, 177.7, 175.8, 48.1, 45.1, 31.6, 24.9, 20.1, 19.1.

(*R*)-2-(1-Benzyl-2,5-dioxopyrrolidin-3-yl)-2-methylpropanal (9d)[13b]

Following the general procedure gave **9d** (70.00 mg, 90%) as colorless prisms; 82% ee.

HPLC (Chiralpak AD-H, 210 nm, *n*-hexane–*i*-PrOH, 80:20, 1.0 mL/min): t_R = 8.0 (minor), 17.0 min (major).

^{1}H NMR: δ = 9.49 (s, 1 H), 7.39–7.27 (m, 5 H), 4.72–4.57 (m, 2 H), 3.03 (dd, *J* = 9.4, 5.4 Hz, 1 H), 2.82 (dd, *J* = 18.3, 9.4 Hz, 1 H), 2.45 (dd, *J* = 18.3, 5.4 Hz, 1 H), 1.17 (s, 3 H), 1.16 (s, 3 H).

^{13}C NMR: δ = 202.81, 177.55, 175.48, 135.77, 128.83, 128.77, 128.10, 48.17, 45.05, 42.59, 31.60, 20.08, 19.23.

(*R*)-2-[1-(4-Bromophenyl)-2,5-dioxopyrrolidin-3-yl]-2-methylpropanal (9e)[14]

Following the general procedure gave **9e** (68.07 mg, 70%) as colorless prisms; 87% ee.

HPLC (Chiralpak OD-H, 230 nm, *n*-hexane–*i*-PrOH, 75:25, 0.9 mL/min): t_R = 30.7 (minor), 52.3 min (major).

^{1}H NMR: δ = 9.48 (s, 1 H), 7.65–7.50 (m, 2 H), 7.22–7.12 (m, 2 H), 3.10 (dd, *J* = 9.5, 5.5 Hz, 1 H), 2.96 (dd, *J* = 18.2, 9.5 Hz, 1 H), 2.61 (dd, *J* = 18.2, 5.5 Hz, 1 H), 1.35 (s, 3 H), 1.28 (s, 3 H).

^{13}C NMR: δ = 202.80, 176.70, 174.51, 132.48, 130.94, 128.19, 122.70, 48.83, 45.12, 32.11, 20.62, 20.08.

(*R*)-2-[1-(3-Chlorophenyl)-2,5-dioxopyrrolidin-3-yl]-2-methylpropanal (9f)[14]

Following the general procedure gave **9f** (77.20 mg, 92%) as colorless prisms; 87% ee.

HPLC (Chiralcel OD-H, 210 nm, *n*-hexane–*i*-PrOH, 75:25, 0.6 mL/min): t_R = 24.0 (minor), 28.1 min (major).

^{1}H NMR: δ = 9.48 (s, 1 H), 7.44–7.31 (m, 2 H), 7.21 (m, 2 H), 3.11 (dd, *J* = 9.5, 5.5 Hz, 1 H), 2.96 (dd, *J* = 18.2, 9.5 Hz, 1 H), 2.65–2.57 (dd, *J* = 18.2, 9.5 Hz, 1 H), 1.35 (s, 3 H), 1.27 (s, 3 H).

^{13}C NMR: δ = 202.8, 176.6, 174.4, 134.7, 132.9, 130.2, 128.9, 126.9, 124.8, 48.7, 45.0, 32.0, 20.5, 19.9.

(*R*)-2-[1-(4-Chlorophenyl)-2,5-dioxopyrrolidin-3-yl]-2-methylpropanal (9g)[13b]

Following the general procedure gave **9g** (73.00 mg, 87%) as colorless prisms; 86% ee.

HPLC (Chiralcel OD-H, 210 nm, *n*-hexane–*i*-PrOH, 75:25, 0.9 mL/min): t_R = 22.4 (minor), 37.1 min (major).

^{1}H NMR: δ = 9.49 (s, 1 H), 7.48–7.41 (m, 2 H), 7.29–7.22 (m, 2 H), 3.12 (dd, *J* = 9.5, 5.4 Hz, 1 H), 2.98 (dd, *J* = 18.1, 9.5 Hz, 1 H), 2.62 (dd, *J* = 18.1, 5.4 Hz, 1 H), 1.36 (s, 3 H), 1.29 (s, 3 H).

^{13}C NMR: δ = 202.8, 176.7, 174.6, 134.6, 130.4, 129.5, 127.9, 48.8, 45.1, 32.1, 20.6, 20.0.

(*R*)-1-(2,5-Dioxo-1-phenylpyrrolidin-3-yl)cyclopentanecarbaldehyde (9h)[14]

Following the general procedure gave **9h** (68.37 mg, 84%) as colorless prisms; 89% ee.

HPLC (Chiralcel OD-H, 210 nm, *n*-hexane–*i*-PrOH, 75:25, 0.5 mL/min): t_R = 37.0 (minor), 49.9 min (major).

^{1}H NMR: δ = 9.38 (s, 1 H), 7.50–7.44 (m, 2 H), 7.39 (m, 1 H), 7.33–7.28 (m, 2 H), 3.05 (dd, *J* = 9.6, 5.2 Hz, 1 H), 2.97 (dd, *J* = 17.6, 9.6 Hz, 1 H), 2.59 (dd, *J* = 17.6, 5.2 Hz, 1 H), 2.36–1.73 (m, 8 H).

^{13}C NMR: δ = 202.0, 177.8, 175.2, 132.1, 129.2, 128.7, 126.7, 60.1, 43.2, 33.2, 32.7, 32.2, 25.8.

(*R*)-1-(2,5-Dioxo-1-phenylpyrrolidin-3-yl)cyclohexanecarbaldehyde (9i)[14]

Following the general procedure gave **9i** (76.18 mg, 89%) as colorless prisms; 93% ee.

HPLC (Chiralcel OD-H, 210 nm, *n*-hexane–*i*-PrOH, 75:25, 0.9 mL/min): t_R = 20.1 (minor), 25.6 min (major).

^{1}H NMR: δ = 9.53 (s, 1 H), 7.50–7.42 (m, 2 H), 7.42–7.36 (m, 1 H), 7.31–7.23 (m, 2 H), 3.21 (dd, *J* = 9.5, 5.9 Hz, 1 H), 2.86 (dd, *J* = 18.2, 9.5 Hz, 1 H), 2.66 (dd, *J* = 18.2, 5.9 Hz, 1 H), 1.96–1.84 (m, 3 H), 1.63–1.53 (m, 7 H).

^{13}C NMR: δ = 204.7, 177.2, 175.0, 131.9, 129.2, 128.7, 126.7, 52.2, 42.6, 31.6, 28.6, 28.1, 25.1, 21.4, 21.2.

(*R*)-2-[(*R*)-2,5-Dioxo-1-phenylpyrrolidin-3-yl]-2-phenylpropanal (9j)[12]

Following the general procedure gave **9j** (66.38 mg, 72%) as a colorless oil; dr 6:1; 81% ee.

HPLC (Chiralpak OD-H, 210 nm, *n*-hexane–*i*-PrOH, 80:20, 1 mL/min): t_R = 26.3 (major diastereomer, minor), 44.7 (major diastereomer, major), 24.1 (minor diastereomer, minor), 37.7 min (minor diastereomer, major).

^{1}H NMR: δ (major) = 9.68 (s, 1 H), 7.48–7.35 (m, 2 H), 7.28 (dd, *J* = 3.9, 1.6 Hz, 1 H), 7.09–7.01 (m, 1 H), 3.82 (dd, *J* = 9.4, 4.6 Hz, 1 H), 2.98 (dd, *J* = 18.9, 9.4 Hz, 1 H), 2.52 (dd, *J* = 18.9, 4.6 Hz, 1 H), 1.78 (s, 1 H).

^{13}C NMR: δ (minor) = 201.03, 176.77, 174.76, 138.03, 132.00, 129.51, 129.29, 128.82, 128.53, 127.31, 126.75, 56.49, 46.63, 32.72, 19.59.

^{1}H NMR: δ (minor) = 9.78 (s, 1 H), 7.50–7.33 (m, 6 H), 7.30–7.18 (m, 5 H), 3.44 (dd, *J* = 9.2, 6.0 Hz, 1 H), 2.65 (ddd, *J* = 24.4, 18.5, 7.6 Hz, 2 H), 1.84 (s, 3 H).

^{13}C NMR: δ (minor) = 199.19, 176.70, 174.75, 135.68, 131.64, 129.53, 129.22, 128.82, 128.69, 127.56, 126.49, 77.58, 77.16, 76.74, 56.05, 45.08, 32.18, 16.64.

(*R*)-2-[(*R*)-2,5-Dioxo-1-phenylpyrrolidin-3-yl]propanal (9k)[13b]

Following the general procedure gave **9k** (34.01 mg, 49%) as a colorless oil; dr 2:1; 72% ee and 60% ee.

HPLC (Chiralpak AD-H, 210 nm, *n*-hexane–*i*-PrOH, 80:20, 0.8 mL/min); t_R = 18.9 (major diastereomer, minor), 21.0 (major diastereomer, major), 24.1 (major diastereomer, minor) 31.0 min (major diastereomer, major).

^{1}H NMR: δ = 9.70*/9.61 (s, 1 H), 7.53–7.28 (m, 10 H), 3.40/3.27* (m, 1 H), 3.17*/3.07 (m, 1 H), 3.02*/2.92 (dd, *J* = 18.5, 9.6 Hz, 1 H), 2.59/2.53* (dd, *J* = 17.9, 5.5 Hz, 1 H), 1.38/1.33* (d, *J* = 7.8 Hz, 3 H).

^{13}C NMR: δ = 201.9/201.5*, 177.8/117.7*, 175.3/175.2*, 132.1/131.8*, 129.3 (2), 128.9*/128.8, 126.7/126.5*, 47.1*/46.6, 40.9/39.6*, 31.7, 11.5/9.8*.

Computational Methods

The structures were initially optimized by using density functional theory (DFT) with the B3LYP[21] as implemented in Gaussian 09,[22] combined with the 6-31G** basis set. Further re-optimization at M06-2X/6-311++G** level of theory[23] were carried out, including polarization functions for a better description of the hydrogen bond activations, and also to account for the important dispersion forces in such large systems. Besides, solvation factors were introduced with the CPCM method,[24] using CH_2Cl_2 or water as indicated in the text and figures, in an attempt to resemble the experimental conditions as closely as possible, since the results are highly dependent on the reaction medium.

The stationary points were characterized by frequency calculations in order to verify that they have the right number of imaginary frequencies.

The intrinsic reaction coordinates (IRC)[25] were followed to verify the energy profiles connecting each TS to the correct associated local minima.

Acknowledgment

The Spanish Ministerio de Ciencia e Innovación (MICINN) (projects CTQ2010-20387, and Consolider Ingenio 2010, CSD2007-00006), the Spanish Ministerio de Economia y Competitividad (MINECO) (projects CTQ2013-43446-P and CTQ2014-51912-REDC), FEDER, the Generalitat Valenciana (PROMETEO 2009/039 and PROMETEOII/2014/017), the Basque Government (GV Grant IT-291-07), the FP7 Marie Curie Actions of the European Commission via the ITN ECHONET network (MCITN-2012-316379), and the Universities of Alicante and Basque Country are gratefully acknowledged for financial support. We also thank SGIker (UPV-EHU) for allocation of computational resources.

Supporting Information

Supporting information for this article is available online at http://dx.doi.org/10.1055/s-0034-1380718.

References

(1) List, B.; Lerner, R. A.; Barbas, C. F. III *J. Am. Chem. Soc.* **2000**, *122*, 2395.
(2) Ahrendt, K. A.; Borthes, C. J.; MacMillan, D. W. C. *J. Am. Chem. Soc.* **2000**, *122*, 4243.
(3) (a) Wagner, J.; Lerner, R. A.; Barbas, C. F. III *Science (Washington, D.C.)* **1995**, *270*, 1797. (b) Barbas, C. F. III; Heine, A.; Zhong, G.; Hoffmann, T.; Gramatikowa, S.; Bjornestedt, R.; List, B.; Anderson, J.; Stura, E. A.; Wilson, E. A.; Lerner, R. A. *Science (Washington, D.C.)* **1997**, *278*, 2085. (c) Zhong, G.; Hoffmann, T.; Lerner, R. A.; Danishefsky, F.; Barbas, C. F. III *J. Am. Chem. Soc.* **1997**, *119*, 8131. (d) Barbas, C. F. III *Angew. Chem. Int. Ed.* **2008**, *47*, 42.
(4) For recent reviews, see: (a) Desmarchelier, A.; Coeffard, V.; Moreau, X.; Greck, C. *Tetrahedron* **2014**, *70*, 2491. (b) Tsakos, M.; Kokotos, C. G. *Tetrahedron* **2013**, *69*, 10199. (c) Serdyuk, O. V.; Heckel, C. M.; Tsogoeva, S. B. *Org. Biomol. Chem.* **2013**, *11*, 7051.
(5) Sánchez, D.; Bastida, D.; Burés, J.; Isart, C.; Pineda, O.; Vilarrasa, J. *Org. Lett.* **2012**, *14*, 536.
(6) Kempf, B.; Hampel, N.; Ofial, A. R.; Mayr, H. *Chem. Eur. J.* **2003**, *9*, 2209.
(7) (a) Taylor, M. S.; Jacobsen, E. N. *Angew. Chem. Int. Ed.* **2006**, *45*, 1520. (b) Yu, X.; Wang, W. *Chem. Asian J.* **2008**, *3*, 516. (c) *Science of Synthesis, Asymmetric Organocatalysis 1, Lewis Base and Acid Catalysts*; List, B., Ed.; Thieme: Stuttgart, **2012**.
(8) Sigman, M. S.; Jacobsen, E. N. *J. Am. Chem. Soc.* **1998**, *120*, 4901.
(9) Schreiner, P. R.; Wittkopp, A. *Org. Lett.* **2002**, *4*, 217.
(10) Okino, T.; Hoashi, Y.; Takemoto, Y. *J. Am. Chem. Soc.* **2003**, *125*, 12672.

(11) Chauhan, P.; Kaur, J.; Chimni, S. S. *Chem. Asian J.* **2013**, *8*, 328.
(12) Kokotos, C. G. *Org. Lett.* **2013**, *15*, 2406.
(13) (a) Yu, F.; Yin, Z.; Huang, H.; Ye, T.; Liang, X.; Xe, J. *Org. Biomol. Chem.* **2010**, *8*, 4767. (b) Bai, J.-F.; Peng, L.; Wang, L.-l.; Wang, L.-X.; Xu, X.-Y. *Tetrahedron* **2010**, *66*, 8928.
(14) Ma, Z.-W.; Liu, Y.-X.; Li, P. L.; Ren, H.; Zhu, Y.; Tao, J.-C. *Tetrahedron: Asymmetry* **2011**, *22*, 1740.
(15) (a) Ávila, A.; Chinchilla, R.; Nájera, C. *Tetrahedron: Asymmetry* **2012**, *23*, 1625. (b) Ávila, A.; Chinchilla, R.; Gómez-Bengoa, E.; Nájera, C. *Eur. J. Org. Chem.* **2013**, 5085.
(16) Ávila, A.; Chinchilla, R.; Gómez-Bengoa, E.; Nájera, C. *Tetrahedron: Asymmetry* **2013**, *24*, 1531.
(17) Flores-Ferrándiz, J.; Chinchilla, R. *Tetrahedron: Asymmetry* **2014**, *25*, 1091.
(18) (a) Almaşi, D.; Alonso, D. A.; Gómez-Bengoa, E.; Nájera, C. *J. Org. Chem.* **2009**, *74*, 6163. (b) Gómez-Torres, E.; Alonso, D. A.; Gómez-Bengoa, E.; Nájera, C. *Org. Lett.* **2011**, *13*, 6106. (c) Gómez-Torres, E.; Alonso, D. A.; Gómez-Bengoa, E.; Nájera, C. *Eur. J. Org. Chem.* **2013**, 1434. (d) Trillo, P.; Baeza, A.; Nájera, C. *Synthesis* **2014**, *46*, 3399.
(19) Vizcaíno-Milla, P.; Sansano, J. M.; Nájera, C.; Fiser, B.; Gómez-Bengoa, E. *Eur. J. Org. Chem.* **2015**, 2614.
(20) (a) Seebach, D.; Golinski, J. *Helv. Chim. Acta* **1981**, *64*, 1413. (b) Seebach, D.; Beck, A. K.; Golinski, J.; Hay, J. N.; Laube, T. *Helv. Chim. Acta* **1985**, *68*, 162.
(21) (a) Lee, C.; Yang, W.; Parr, R. G. *Phys. Rev. B* **1988**, *37*, 785. (b) Becke, A. D. *J. Chem. Phys.* **1993**, *98*, 5648. (c) Kohn, W.; Becke, A. D.; Parr, R. G. *J. Phys. Chem.* **1996**, *100*, 12974.
(22) Frisch, M. J.; Trucks, G. W.; Schlegel, H. B.; Scuseria, G. E.; Robb, M. A.; Cheeseman, J. R.; Scalmani, G.; Barone, V.; Menucci, B.; Petersson, G. A.; Nakatsuji, H.; Caricato, M.; Li, X.; Hratchian, H. P.; Izmaylov, A. F.; Bloino, J.; Zheng, G.; Sonnenberg, J. L.; Hada, M.; Ehara, M.; Toyota, K.; Fukuda, R.; Hasegawa, J.; Ishida, M.; Nakajima, T.; Honda, Y.; Kitao, O.; Nakai, H.; Vreven, T.; Montgomery, J. A. Jr.; Peralta, J. E.; Ogliaro, F.; Bearpark, M.; Heyd, J. J.; Brothers, E.; Kudin, K. N.; Staroverov, V. N.; Kobayashi, R.; Normand, J.; Raghavachari, K.; Rendell, A.; Burant, J. C.; Iyengar, S. S.; Tomasi, J.; Cossi, M.; Rega, N.; Millam, J. M.; Klene, M.; Knox, J. E.; Cross, J. B.; Bakken, V.; Adamo, C.; Jaramillo, J.; Gomperts, R.; Stratmann, R. E.; Yazyev, O.; Austin, A. J.; Cammi, R.; Pomelli, C.; Ochterski, J. W.; Martin, R. L.; Morokuma, K.; Zakrewski, V. G.; Voth, G. A.; Salvador, P.; Dannenberg, J. J.; Dapprich, S.; Daniels, A. D.; Farkas, O.; Foresman, J. B.; Ortiz, J. V.; Cioslowski, J.; Fox, D. J. *Gaussian 09, Revision D.01*; Gaussian Inc: Wallingford (CT, USA), **2013**.
(23) Zhao, Y.; Truhlar, D. G. *Theor. Chem. Acc.* **2008**, *120*, 215.
(24) (a) Cancès, E.; Mennucci, B.; Tomasi, J. *J. Chem. Phys.* **1997**, *107*, 3032. (b) Tomasi, J.; Mennucci, B.; Cancès, E. *J. Mol. Struct.: THEOCHEM* **1999**, *464*, 211.
(25) González, C.; Schlegel, H. B. *J. Phys. Chem.* **1990**, *94*, 5523.